Figures 1a–1f show the dimensionless distribution of free-surface height for $R_m = 0.5$ and different values of B. The effects of the contact angle θ may be seen by comparison of Figs. 1b and 1c. The effects of Weber number on the dimensionless meniscus height $F(1)$ are shown in Fig. 2 for different values of R_m; the limiting Weber numbers are also indicated. Figure 3 shows the effects of Bond numbers on the meniscus height for $\theta = 15°$, $R_m = 0.5$, and different values of W. The meniscus heights for the static case are given in Fig. 4.

The following conclusions may be drawn from Figs. 1–4: 1) surface velocities have strong effects on liquid free-surface shape and meniscus height; 2) the relative effect of Weber number on the meniscus height decreases as the Bond number increases; and 3) for the velocity distributions selected, the meniscus height increases for most cases as the Weber number is increased (there are exceptions, e.g., for the case with $B = 0$, $\theta = 75°$, and $R_m = 0.75$).

Reference

[1] Chin, J. H., et al., "Theoretical and experimental studies of zero-g heat transfer modes," Lockheed Missiles and Space Co., Monthly Progr. Rept., NASA Contract NAS 8-11525 (November–December 1963).

Influence of Magnetic Fields upon Separation

William H. Heiser*
Massachusetts Institute of Technology, Cambridge, Mass.

It is well known that rotational motion of a conductor is resisted by induced currents if a magnetic field not parallel to the axis of rotation is applied. For example, a solid cylindrical shell of arbitrary thickness and diameter set spinning initially with angular velocity ω_0 in the presence of a transverse magnetic field B_0 (Fig. 1) can be shown to slow down in accordance with the equation

$$\omega(t) = \omega_0 \exp\{-(\sigma B_0{}^2/2\rho)t\}$$

provided that ρ and σ are constant throughout the material, $D_0 \ll H$, and $\mu_0\sigma\omega_0 D_0{}^2$ (the magnetic Reynolds number) $\ll 1$. The striking magnitude of this effect is indicated by the result that the time required for a copper shell to slow to $\frac{1}{10}$ of its initial rotational speed $(4.6\rho/\sigma B_0{}^2)$ in the presence of a transverse field of 1 w/m^2 is only $\sim 10^{-3}$ sec. The resistance to radial current flow causes the decay time to increase as D_0/H increases.

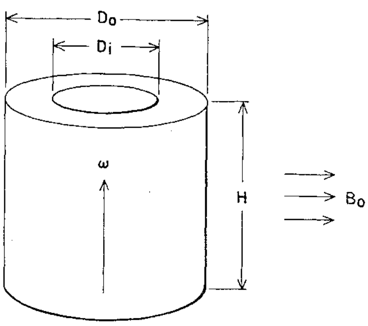

Fig. 1 Solid cylindrical shell spinning in transverse magnetic field.

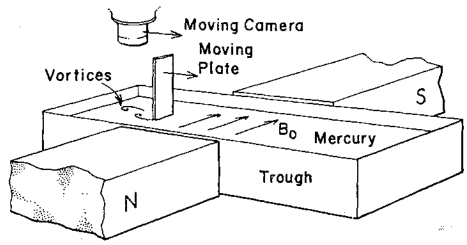

Fig. 2 Schematic representation of the experiment.

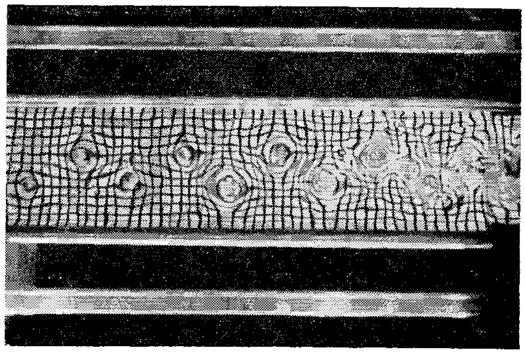

Fig. 3 Vortex street generated in the magnetic field-free region at the start of the run.

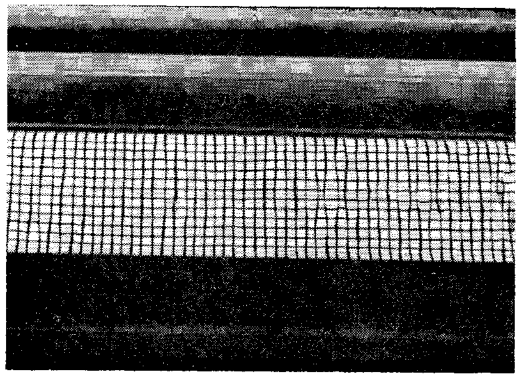

Fig. 4 No vortex street can be observed within the region of transverse magnetic field.

Experiments were conducted to demonstrate this effect upon the Kármán vortex street generated by a flat plate moving with constant velocity through still mercury (Fig. 2) at the studios of Educational Services Inc., Watertown, Mass. The experiments were photographed from above as a grid, with an apparent spacing approximately the diameter of the individual vortices, was reflected from the mercury surface. This technique made the small surface dimples caused by the rotating mercury quite visible as distortions of the regular grid pattern.

Figures 3–5 are three consecutive photographs of the reflected grid pattern taken during a single constant velocity run from left to right, the flat plate being at the extreme right in each photograph. Figure 3 shows clearly the vortex street generated outside the region of transverse magnetic field. Figure 4 gives no indication that vortices are ever generated within the region of magnetic field. Figure 5 shows the resumption of the vortex street in the region where the magnetic field fringes. For the experiment shown in

Received July 16, 1964. These experiments were performed for the film "Magnetohydrodynamics" by J. A. Shercliff, produced by Educational Services Inc. for the National Committee for Fluid Mechanics Films, with the financial support of the National Science Foundation.

* Assistant Professor of Mechanical Engineering.

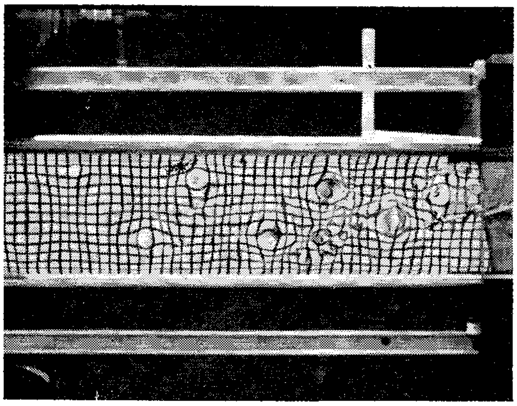

Fig. 5 The vortex street resumes in the magnetic field-free region at the end of the run.

these photographs, Reynolds number (based upon flat-plate width) $\sim 10^4$, magnetic Reynolds number (based upon flat-plate width) $\sim 10^{-3}$, vortex decay time $(4.6\rho/\sigma B_0^2) \sim 1$ sec, and vortex $D_0/H \sim 1$.

Despite the fact that the vortex decay time was long enough to allow observation of the persisting vortices, none can be seen in the magnetic field region of this experiment.

Vortices could only be observed within the magnetic field region when the vortex decay time was increased to ~ 5 sec. In accordance with the notion that the transverse magnetic field suppresses the rotation of existing vortices, the vortices observed within the magnetic field in this case did die out much more rapidly than those found outside the magnetic field.

These observations indicate that the stronger transverse magnetic field did more than merely suppress the vortices created by the flat plate, but that the magnetic field altered the separation characteristics of the boundary layer to prevent the formation of the vortex street. Although a complete solution of the problem is difficult, the Kármán-Pohlhausen technique can be used to determine whether magnetohydrodynamic effects are large enough to possibly influence separation.[1]

Since the still mercury can impress the condition of zero electric field upon the thin boundary layer, the current density at the wall of the moving flat plate must be nearly $\sigma_0 U_0 B_0$, where U_0 is the plate velocity. Consequently, the momentum equation at the plate wall becomes approximately

$$\nu\left(\frac{\partial^2 u}{\partial y^2}\right)_0 = -U_0\frac{dU}{dx} - \frac{\sigma U_0 B_0^2}{\rho}$$

and the resulting shape factor Λ' is, therefore, related to the conventional shape factor $\Lambda = (\delta^2/\nu)(dU/dx)$ through the expression

$$\Lambda' = \Lambda\{1 + \sigma B_0^2/\rho(dU/dx)\}$$

Note that $\Lambda' \geq \Lambda$ because the induced currents tend to fill out the velocity profile and that separation still occurs when $\Lambda' = -12$. For the experiment just described, $\sigma B_0^2/[\rho(dU/dx)] \sim -1$, indicating that the effect of the induced currents in the boundary layer upon separation cannot be neglected for this case. Furthermore, the Hartmann number (based upon flat-plate width) for this experiment was approximately 100, which means that the magnetohydrodynamic forces will tend to decrease the absolute value of Λ' by reducing δ.

The results of these experiments, therefore, appear to be quantitatively in accord with boundary-layer theory, and they demonstrate that magnetic fields can exert a strong influence upon boundary-layer separation. It was also experimentally demonstrated that a magnetic field transverse to the axis of a two-dimensional, wide-angle diffuser could prevent boundary-layer separation.

Reference

[1] Schlichting, H., *Boundary Layer Theory* (McGraw-Hill Book Co., Inc., New York, 1960), 4th ed., Chap. 12, p. 243.

Three-Dimensional Symmetric Vortex Flow

Ajit Kumar Ray*

Department of Transport, Government of Canada, Ottawa, Canada

Many problems of interest in missile or aircraft aerodynamics require a detailed knowledge of the vortex flow due to bodies of revolution or lifting surfaces, and in the following the behavior of symmetrical vortex pattern in the presence of a semicircular section in the crossflow plane has been explored with the help of a simplified model in which the vorticity is moving along the feeding sheets into the cores at all times.

Symmetric vortex separation is exactly identified in the two-dimensional picture of the wake development behind a circular cylinder. The boundary layer separates from the surface of the cylinder at the rearward stagnation point, and the two separation points move symmetrically away from this point around the cylinder. When these boundary-layer separation points reach a certain angular distance from the rearward point, the two regions of vorticity break away from the boundary layer and proceed downstream, forming the wake. Depending upon the Reynolds number, the flow behind the cylinder in the wake is identified as the Stokes flow (without the wake formation), symmetric vortex shedding and anti symmetric vortex formation with rapid transgress into turbulent motion in the wake.

In the three-dimensional flow, the forementioned vortex separation is observed on the leeward side of the slender bodies of revolution at a comparatively large angle of attack in the subsonic to supersonic range. If we imagine a fixed plane in the fluid perpendicular to the axis of the body of revolution, then the body pierces the plane with a velocity $U \sin\alpha$, α being the local body angle of attack and U the velocity. Now, considering the case in which the expanding circle, as the nose pierces the plane, changes slowly with x, x being taken in the direction of the body axis, the flow in the crossflow plane can be looked upon as the two-dimensional one. Such a procedure will not be invalid in view of the conical flow assumption in the slender body theory.

In the present problem of flow past a half cone, the flow in the crossflow plane can be solved by choosing a suitable transformational function that will map the flow plane conformally past the semicircle section into the flow in the crossflow plane past a circular section.[1] Designating the physical plane (i.e., the semicircle plane) by the Z plane and the transformed plane (i.e., the circle plane) by the τ plane, the appropriate transformation mapping the flow conformally between the two planes is given by

$$\left(\frac{Z - 3(3)^{1/2}a/4}{Z + 3(3)^{1/2}a/4}\right) = \left(\frac{\tau - ae^{-i\pi/6}}{\tau + ae^{i\pi/6}}\right)^{3/2} \quad (1)$$

where C, the center of the circle, has been taken as the origin in the τ plane, and infinity has been preserved during the transformation in both planes.[1]

Received July 16, 1964.

* Employee. Member AIAA.